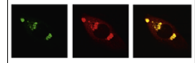


Available online at www.sciencedirect.com
www.elsevier.com/locate/brainres

Brain Research



Research Report

Estradiol rapidly modulates synaptic plasticity of hippocampal neurons: Involvement of kinase networks

Yoshitaka Hasegawa^{a,1}, Yasushi Hojo^{a,b,c,1}, Hiroki Kojima^a, Muneki Ikeda^a, Keisuke Hotta^a, Rei Sato^a, Yuuki Ooishi^a, Miyuki Yoshiya^a, Bon-Chu Chung^c, Takeshi Yamazaki^e, Suguru Kawato^{a,b,c,d,*}

^aDepartment of Biophysics and Life Sciences, Graduate School of Arts and Sciences, University of Tokyo, Komaba 3-8-1, Meguro, Tokyo 153, Japan

^bBioinformatics Project of Japan Science and Technology Agency, University of Tokyo, Tokyo, Japan

^cInternational Collaboration Project (Japan–Taiwan) of Japan Science and Technology Agency, University of Tokyo, Tokyo, Japan; Institute of Molecular Biology, Academia Sinica, Taipei, Taiwan

^dProject of Special Coordinate Funds for Promoting Science and Technology of Ministry of Education, Science and Technology, University of Tokyo, Tokyo, Japan

^eLaboratory of Molecular Brain Science, Graduate School of Integrated Arts and Sciences, Hiroshima University, Higashi–Hiroshima, Japan

ARTICLE INFO

Article history:

Accepted 27 December 2014

Available online 13 January 2015

Keywords:

Estradiol

Estrogen

Estrogen receptor

LTP

Spine

Synaptic plasticity

Kinase

Rapid action

ABSTRACT

Estradiol (E2) is locally synthesized within the hippocampus in addition to the gonads. Rapid modulation of hippocampal synaptic plasticity by E2 is essential for synaptic regulation. Molecular mechanisms of modulation through synaptic estrogen receptor (ER) and its downstream signaling, however, have been still unknown.

We investigated induction of LTP by the presence of E2 upon weak theta burst stimulation (weak-TBS) in CA1 region of adult male hippocampus. Since only weak-TBS did not induce full-LTP, weak-TBS was sub-threshold stimulation. We observed LTP induction by the presence of E2, after incubation of hippocampal slices with 10 nM E2 for 30 min, upon weak-TBS. This E2-induced LTP was blocked by ICI, an ER antagonist. This E2-LTP induction was inhibited by blocking Erk MAPK, PKA, PKC, PI3K, NR2B and CaMKII, individually, suggesting that Erk MAPK, PKA, PKC, PI3K and CaMKII may be involved in downstream signaling for activation of NMDA receptors. Interestingly, dihydrotestosterone suppressed the E2-LTP.

We also investigated rapid changes of dendritic spines (=postsynapses) in response to E2, using hippocampal slices from adult male rats. We found 1 nM E2 increased the density of spines by approximately 1.3-fold within 2 h by imaging Lucifer Yellow-injected CA1 pyramidal neurons. The E2-induced spine increase was blocked by ICI. The increase in

*Corresponding author at. Department of Biophysics and Life Sciences, Graduate School of Arts and Sciences, University of Tokyo, Komaba 3-8-1, Meguro, Tokyo 153, Japan. Fax: +81 3 5454 6517.

E-mail address: kawato@bio.c.u-tokyo.ac.jp (S. Kawato).

¹Contributed equally to the present work.

spines was suppressed by blocking PI3K, Erk MAPK, p38 MAPK, PKA, PKC, LIMK, CaMKII or calcineurin, individually. On the other hand, blocking JNK did not inhibit the E2-induced spine increase.

Taken together, these results suggest that E2 rapidly induced LTP and also increased the spine density through kinase networks that are driven by synaptic ER.

This article is part of a Special Issue entitled *SI: Brain and Memory*.

© 2015 Elsevier B.V. All rights reserved.

1. Introduction

Finding of local synthesis of estrogen and androgen in the adult male/female hippocampus opened a new field of estrogen function in relation to the regulation of daily memory formation (Kimoto et al., 2001; Kawato et al., 2002, 2003; Hojo et al., 2004; Kretz et al., 2004; Hojo et al., 2008; Okamoto et al., 2012; Kato et al., 2013). The level of adult male hippocampal estradiol (E2) is higher (~8 nM) than that of plasma E2 (~0.01 nM), as determined by mass-spectrometric analysis (Hojo et al., 2009). Therefore, it is important to investigate modulation effects by hippocampal E2 on synaptic plasticity.

In addition to slow modulation effects on synaptic plasticity by circulating E2, E2 exerts rapid (1–2 h) influence on the synaptic plasticity of rat hippocampal glutamatergic neurons in slices, as has been demonstrated by a number of electrophysiological investigations in rats and mice, concerning the long-term potentiation (LTP) in CA1 (Foy et al. 1999; Bi et al., 2000), the long-term depression (LTD) in CA1 (Vouimba et al., 2000; Mukai et al., 2007) and kainate current in CA1 (Gu and Moss, 1996; Gu et al., 1999).

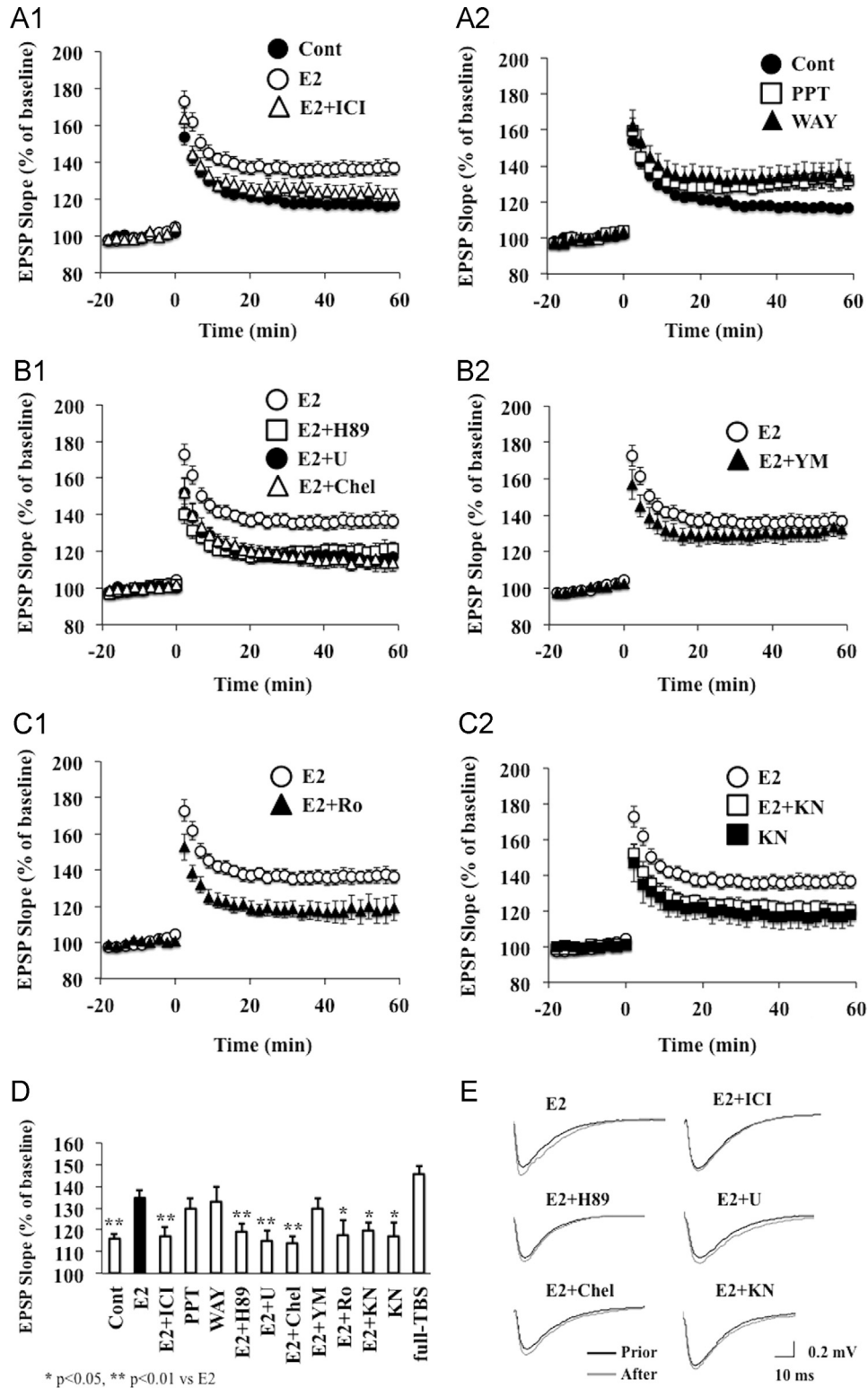
The rapid effect of E2 may be driven through either ER α or ER β , possibly localized at the membrane, in analogy with cultured cells of peripheral origin (McEwen and Alves, 1999; Razandi et al., 1999). It is probable that synaptically localized ER α or ER β (Milner et al., 2005; Mukai et al., 2007, 2010; Hojo et al., 2008) may participate in rapid modulation by E2. Involvement of non-ER α or non-ER β type receptor, however, might not be excluded (Gu and Moss, 1996; Gu et al., 1999).

On the other hand, extensive studies have been performed to investigate the role of E2 in slowly (1–4 days) modulating hippocampal plasticity, because the hippocampus is known to

be a target for the actions of gonadal estrogens reaching the brain via blood circulation. For example, the density of dendritic spines in the CA1 pyramidal neurons is modulated *in vivo* by supplement of E2 in ovariectomized (OVX) animals (Gould et al., 1990; Woolley et al., 1990; Woolley and McEwen, 1992; Leranth et al., 2000, 2002), resulting in increase/recovery the number of spines. *In vitro* investigations have also shown that spine density is increased following several days' treatment of cultured hippocampal slices with E2 (Murphy and Segal, 1996; Pozzo-Miller et al., 1999). Other type of E2 effects on synaptic receptors of the hippocampal neurons has also been accumulated, including an NMDA receptor-dependent mechanism of E2 regulation on dendritic spine density (Woolley and McEwen, 1994), and increase of glutamate binding to NMDA receptors by E2 (Woolley et al., 1997). LTP study of slow/genomic effects shows E2-induced enhancement of LTP after 24–48 h of E2 injection to OVX rats (Smith et al., 2002).

The current study was designed, using acute hippocampal slices from adult male rats, to investigate (1) kinase dependence of signaling mechanisms in rapid modulation of E2-induced LTP upon weak theta burst stimulation (weak-TBS) and (2) kinase dependence of E2-induced rapid spinogenesis. Selective blockers of many kinases were used. In order to investigate E2-induced LTP, slices were incubated with E2, and weak-TBS was applied. These weak-TBS methods were employed, because E2 application does not enhance tetanus-induced LTP in 3 month-old adult rat hippocampus (Ooishi et al., 2012b), since strong tetanus probably saturates LTP.

Fig. 1 – E2 induces LTP upon weak-TBS in the CA1 hippocampal slices. (A1) Slices with 0 nM E2 (Cont) (closed circle, n=10 slices), with 10 nM E2 (E2) (open circle, n=10 slices), with 10 nM E2 plus 100 nM ICI (E2+ICI) (open triangle, n=8 slices). (A2) Slices with 0 nM E2 (Cont), with 100 nM PPT (PPT) (open square, n=8 slices), with 100 nM WAY-200070 (WAY) (closed triangle, n=8 slices). Vertical axis indicates EPSP slope. Here, 100% refers to the EPSP slope value of the average of t = -9 to 0 min prior to weak-TBS stimulation. LTP was induced at time t=0. Illustrated data points and error bars represent the mean \pm SEM from n of independent slices. (B1) Effect of kinase inhibitors. Co-incubation of E2 with PKA inhibitor H89 (10 μ M) prevented the induction of LTP (E2+H89) (open square, n=8 slices), with MAPK inhibitor U0126 (10 μ M) prevented the induction of LTP (E2+U) (closed circle, n=8 slices), with PKC inhibitor chelerythrine (10 μ M) prevented the induction of LTP (E2+Chel) (open triangle, n=8 slices). (B2) Co-incubation of E2 with mGluR1 inhibitor YM202074 (4 μ M) did not prevent the induction of LTP (E2+YM) (closed triangle, n=8 slices). (C1) NR2B inhibitor Ro25-6981 (1 μ M) suppressed the E2-LTP (E2+Ro) (closed triangle, n=8 slices). (C2) CaMKII inhibitor KN-93 (20 μ M) suppressed the E2-LTP (E2+KN) (open square, n=8 slices). Perfusion of only KN (20 μ M) did not change the induction of the small LTP upon weak-TBS (KN) (closed square, n=5 slices). (D) Comparison of inhibitor-induced modulation effects on E2-LTP as shown in (A), (B) and (C) Light most is full-LTP induced by full-TBS (full-TBS). Statistical significance was defined as * p < 0.05, ** p < 0.01. (E) Representative raw traces of EPSP, showing sample recordings prior to (black line) or after (gray line) weak-TBS stimulation.



2. Results

2.1. Estradiol induces LTP (E2-LTP) upon weak-TBS

To investigate the effect of estradiol (E2) incubation on the synaptic transmission, we investigated LTP upon weak-TBS (15 pulses) in CA1 of the adult hippocampal slices. In the absence of E2 treatments, weak-TBS (sub-threshold stimulation) induced only small LTP at $t=60$ min with low EPSP ($116\pm 2\%$, $n=10$ slices) (Fig. 1A and D) (Hasegawa et al., 2014). To measure E2 effects, acute slices were incubated for 30 min with 10 nM E2, then weak-TBS was applied. E2 treatments established LTP-induction upon weak-TBS at $t=60$ min ($135\pm 4\%$, $n=10$ slices) (Fig. 1A and D). Co-incubation of ICI (100 nM), an antagonist of ER α / ER β , with E2 completely blocked the E2 effects, resulting in $117\pm 4\%$ for EPSP ($n=8$ slices). It should be noted that the incubation with only ICI did not significantly affect the small LTP upon weak TBS ($120\pm 2\%$, $n=5$ slices) (Fig. S1). In order to selectively activate ER α , slices were incubated for 30 min with 100 nM propyl pyrazole triol (PPT), a selective agonist of ER α . PPT established LTP-induction upon weak-TBS, by increasing EPSP to $130\pm 5\%$ ($n=8$ slices) (Fig. 1A2 and D). In order to selectively activate ER β , slices were incubated for 30 min with 100 nM WAY-200070, a selective agonist of ER β (Kramar et al., 2009) WAY-200070 treatments established LTP-induction upon weak-TBS, by increasing the EPSP to $133\pm 7\%$ ($n=8$ slices) (Fig. 1A2 and D). Application of full-TBS (total 50 pulses) increased EPSP up to $146\pm 4\%$ ($n=8$ slices), implying that the E2-induced LTP (135%) is close to this full-LTP (146%).

To assess the effect of E2 on the presynaptic activation, paired pulse facilitation (PPF) was analyzed. No significant change in the PPF ratio was observed after E2 incubation, suggesting that E2 did not modulate presynapses and that the observed E2-LTP should be due to postsynaptic events.

2.1.1. Kinase inhibitors prevent E2-LTP

Co-incubation of U0126 (10 μ M), an inhibitor of Erk MAPK (Favata et al., 1998; Ooishi et al., 2012b), with E2 considerably suppressed E2-LTP, resulting in decrease of EPSP to $115\pm 5\%$ ($n=8$ slices) (Fig. 1B1 and D). Note that incubation with only U0126 did not change the small LTP upon weak-TBS ($115\pm 4\%$, $n=5$ slices) (Fig. S1). Co-incubation of H89 (10 μ M), an inhibitor of PKA (Chijiwa et al., 1990), with E2 considerably suppressed E2-LTP, resulting in $119\pm 4\%$ ($n=8$ slices) (Fig. 1B1 and D). Incubation with only H89 did not change the small LTP upon weak-TBS ($114\pm 5\%$, $n=5$ slices) (Fig. S1). Co-incubation of chelerythrine (10 μ M), an inhibitor of PKC (Herbert et al., 1990), with E2 considerably suppressed E2-LTP, resulting in LTP magnitude of $114\pm 3\%$ ($n=8$ slices) (Fig. 1B1 and D). Co-incubation of YM202074 (4 μ M), an inhibitor of mGluR1 (Nebieridze et al., 2012), with E2 established LTP-induction by weak-TBS, with EPSP to $130\pm 4\%$ ($n=8$ slices) (Fig. 1B2 and D). Incubation with only chelerythrine and only YM202074 did not change the small LTP upon weak-TBS ($117\text{--}123\%$, $n=5$ slices) (Fig. S1).

Co-incubation of LY294002 (10 μ M), an inhibitor of PI3K, with E2 suppressed E2-LTP resulting in decrease of EPSP to $121\pm 4\%$ ($n=8$ slices), with no effects by LY294002. Incubation

with PP2 (10 μ M), a Src kinase inhibitor, with E2 did not suppress E2-LTP ($128\pm 5\%$, $n=6$ slices).

2.1.2. NR2B antagonist prevents E2-LTP

Co-incubation of Ro25-6981 (1 μ M) (Fischer et al., 1997; Ooishi et al., 2012b), an antagonist of NR2B subunit of NMDA receptors, with E2 considerably suppressed E2-LTP, resulting in decrease of EPSP to $118\pm 7\%$ ($n=8$ slices) (Fig. 1C1 and D). Incubation with only Ro25-6981 did not change the small LTP upon weak-TBS ($122\pm 3\%$, $n=5$ slices) (Fig. S1).

2.1.3. Ca²⁺/Calmodulin-dependent protein kinase II (CaMKII) inhibitor prevents E2-LTP

After incubation of slices with E2 for 30 min, KN-93 (20 μ M) (Ehrlich and Malinow, 2004), an inhibitor of CaMKII, was perfused before weak-TBS. Perfusion of KN-93 considerably suppressed E2-LTP, resulting in decrease of EPSP to $120\pm 4\%$ ($n=8$ slices) (Fig. 1C2 and D). Here, KN-93 suppressed CaMKII, since CaMKII may be activated by elevated Ca²⁺ influx through activated NMDA receptors by E2-incubation. Perfusion of only KN-93 did not change the small LTP upon weak-TBS ($117.3\pm 1.9\%$, $n=5$ slices) (Fig. 1C2 and D).

2.2. Dihydrotestosterone (DHT) suppressed E2-induced LTP upon weak-TBS

We investigated the effect of androgen on E2-induced LTP. Slices were incubated for 30 min with 10 nM E2 plus DHT before application of weak-TBS. Interestingly, co-incubation of DHT (10 nM) with E2 completely blocked the E2-LTP, resulting in decrease of EPSP to $115\pm 3\%$ ($n=9$ slices) (Fig. 2A1 and C). Note that incubation with only DHT did not change the small LTP upon weak-TBS ($121\pm 3\%$, $n=10$ slices) (Fig. 2A2 and C).

Paired pulse facilitation (PPF) was analyzed. No significant change in the PPF ratio was observed after DHT plus E2 incubation, suggesting that DHT did not modulate presynaptic events, and therefore the observed of DHT effects on E2-LTP should be due to postsynaptic events.

2.2.1. Inhibition of AR and phosphatase prevents DHT-induced suppression

Co-incubation of hydroxyflutamide (HF) (1 μ M), an antagonist of AR (androgen receptor), with E2 plus DHT inhibited the DHT-induced suppression, resulting in recovery of EPSP to $143\pm 10\%$ ($n=9$ slices) (Fig. 2B1 and 2C). Incubation with only HF did not affect the small LTP upon weak-TBS ($117\pm 4\%$, $n=6$ slices), nor significantly changed E2-LTP ($132\pm 3\%$, $n=6$ slices) (Fig. S2). HF did not significantly change DHT-EPSP upon weak-TBS ($115\pm 4\%$, $n=6$ slices) (Fig. S2). Co-incubation of cyclosporin A (CsA) (10 μ M), an inhibitor of calcineurin (PP2B) (Wiederrecht et al., 1993), with E2 plus DHT inhibited the suppressive effect of DHT, resulting in recovery of EPSP to $140\pm 10\%$ ($n=6$ slices) (Fig. 2B2 and C). Here, CsA was used to prevent suppression of calcineurin in signaling of “DHT \rightarrow AR \rightarrow calcineurin \rightarrow suppression of NMDA receptors”. Incubation with only CsA did not change the small LTP upon weak-TBS ($116\pm 4\%$, $n=6$ slices) (Fig. S2). CsA did not significantly change E2-LTP ($130\pm 3\%$, $n=6$ slices). CsA did not change DHT-EPSP ($114\pm 5\%$, $n=6$ slices) (Fig. S2).

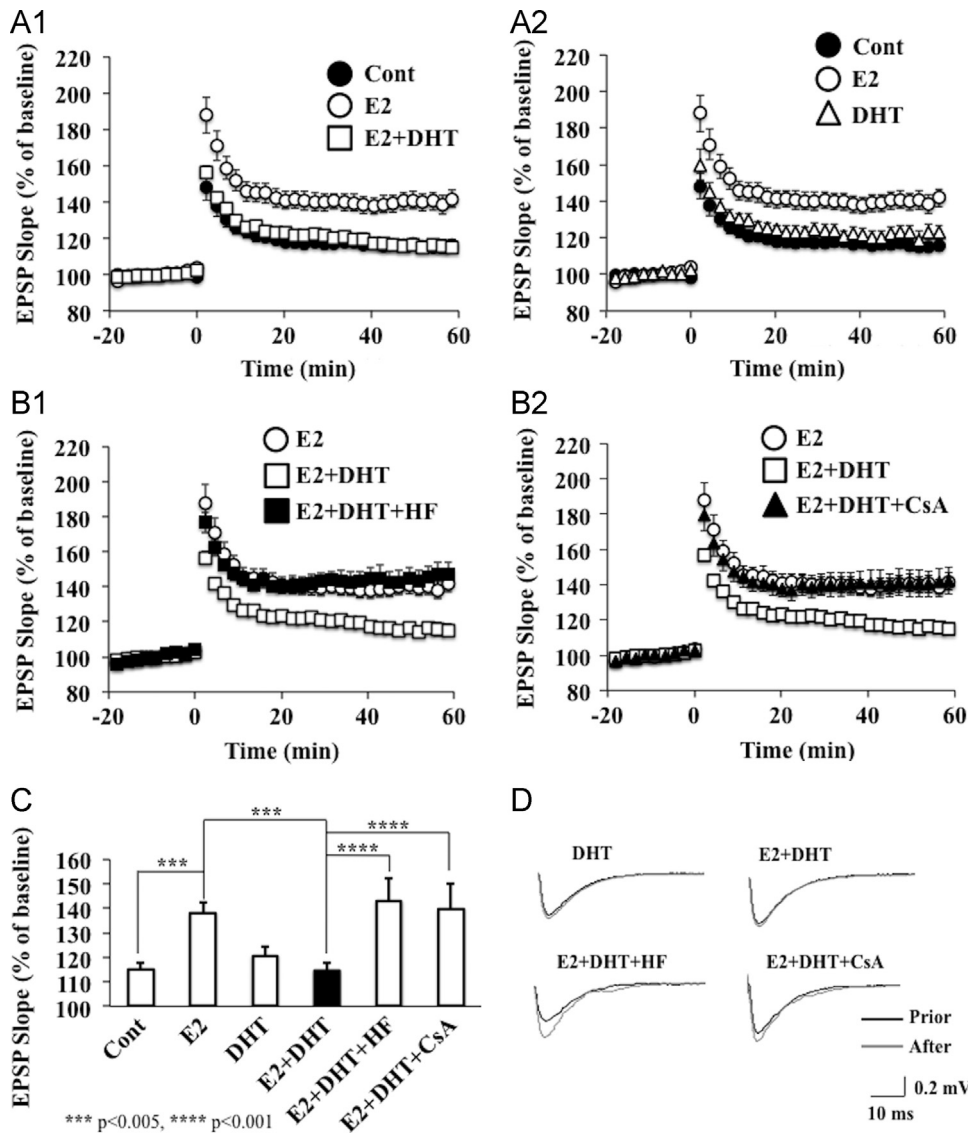


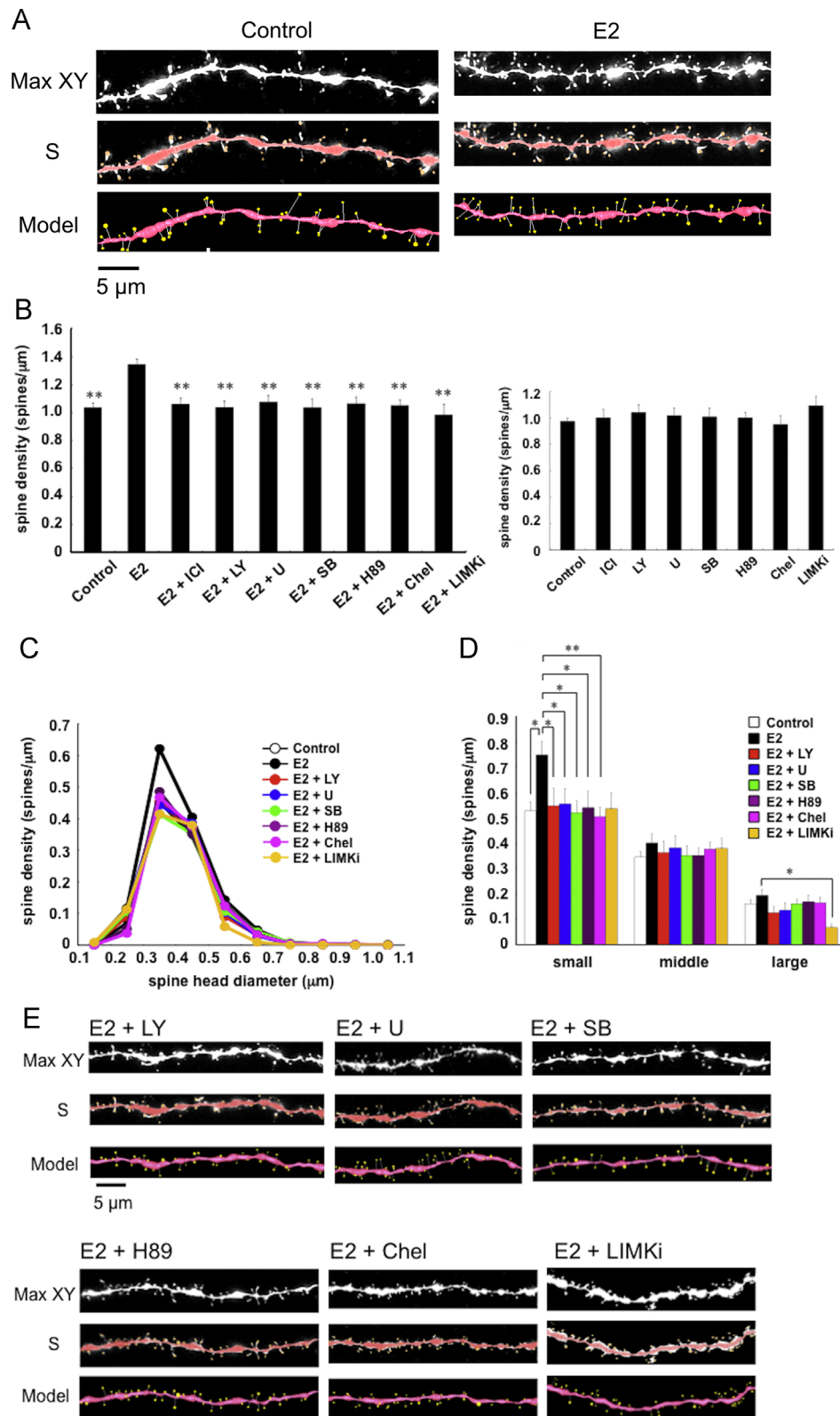
Fig. 2 – DHT suppressed E2-induced LTP upon weak-TBS. (A1) E2-LTP (E2) (open circle, $n=10$ slices) was suppressed when DHT (10 nM) was co-incubated with E2 (10 nM) (E2+DHT) (open square, $n=9$ slices). **(A2)** Only 10 nM DHT without E2 was incubated with slices (DHT) (open, triangle $n=10$ slices). The number of independent experiments is indicated as n . Vertical axis indicates EPSP slope. Here, 100% refers to the EPSP slope value of the average of $t=-9$ to 0 min prior to weak-TBS stimulation. LTP was induced at time $t=0$. Illustrated data points and error bars represent the mean \pm SEM from n of independent slices. **(B1)** AR antagonist HF (1 μ M) prevented the DHT-induced suppression of E2-LTP (E2+DHT+HF) (closed square, $n=9$ slices). **(B2)** Calcineurin inhibitor cyclosporine A (10 μ M) blocked the DHT-induced suppression of E2-LTP (E2+DHT+CsA) (closed triangle, $n=6$ slices). **(C)** Comparison of DHT effects on E2-LTP as shown in (A) and (B). Statistical significance was defined as *** $p<0.005$, **** $p<0.001$. **(D)** Representative raw traces of EPSP, showing sample recordings prior to (black line) or after (gray line) weak-TBS stimulation.

2.3. Rapid effect of E2 on CA1 spinogenesis

We investigated the effect of E2 on the modulation of the dendritic spine density and morphology. Single spine imaging was performed for Lucifer Yellow-injected neurons in hippocampal slices. We analyzed secondary branches of the apical dendrites located 100–200 μ m distant from the pyramidal cell body around the middle of the stratum radiatum of CA1 region.

Following a 0.5–2 h treatments with E2, treated dendrites have significantly more spines than control dendrites (i.e. without E2) (Fig. 3A). Time dependency of E2 treatment was

demonstrated by treating slices for 0.5, 1 and 2 h with 1 nM E2 (Fig. S3). The increasing effect on the total spine density was approximately proportional to the incubation time, showing 1.02 (0.5 h), 1.22 (1 h) and 1.34 spines/ μ m (2 h) in E2-treatments. Dose dependency was also examined after 2 h incubation (Fig. S3). The increasing effect was most significant at 1 nM E2 (1.34 spines/ μ m) compared with 0.1 nM (1.01 spines/ μ m) and 10 nM (1.33 spines/ μ m) E2. Because a 2 h treatment with 1 nM E2 was most effective for spinogenesis, these incubation time and concentration was used in the following investigations unless specified (Fig. S3).



Blocking of estrogen receptor (ER) by 1 μM ICI182, 780 (ICI), a specific inhibitor of ER, completely abrogated the enhancing effect of E2 on the spine density (Fig. 3).

2.3.1. Spine head diameter analysis

The morphological changes in spine head diameter induced by 2 h treatments were assessed. We classified the spines into three categories depending on their head diameter, e.g. 0.2–0.4 μm as small-head spines, 0.4–0.5 μm as middle-head spines, and larger than 0.5 μm as large-head spines (Fig. 3C).

Small-, middle-, and large-head spines may be different in the number of AMPA receptors, and therefore these three types of spines may have different efficiency in signal transduction. The number of AMPA receptors (including GluR1 subunit) in the spine increases as the size of postsynapse increases, whereas the number of NMDA receptors (including NR2B subunit) may be relatively constant (Shinohara et al., 2008).

We performed a statistical analysis based on classification of the spines into three categories. In control slices (without E2), the spine density was 0.52 spines/ μm for small-head spines, 0.35 spines/ μm for middle-head spines, and 0.16 spines/ μm for large-head spines. Upon treatment with E2, the density of small-head spines significantly increased, while the density of middle- and large-head spines was not significantly altered (Fig. 3C and D). The concurrent application of E2 and ICI significantly decreased the density of small-head spines, while the density of middle- and large-head spines was not significantly changed (Fig. 3D).

2.4. Signaling pathways depending on protein kinases (PI3K, Erk MAPK, p38 MAPK, PKA, PKC, LIM kinase (LIMK))

2.4.1. Total density analysis

We investigated intracellular signaling pathways of several kinases involved in the E2-induced spine increase by using

selective inhibitors of kinases (Fig. 3B). Blocking PI3K by 10 μM LY294002, abolished the increase of total spine density induced by E2. Application of 25 μM U0126, Erk MAPK inhibitor, abolished the increasing effect by administration of E2. Application of 10 μM SB203580, a p38 MAPK inhibitor, also prevented the effect by E2. Application of 10 μM H89, an inhibitor of protein kinase A (PKA), blocked the increasing effect by E2. When all subfamilies of protein kinase C (PKC) were blocked by using 10 μM chelerythrine, a non-selective PKC subfamily inhibitor, the increasing effect by E2 on the spine density were blocked. Selective inhibition of only PKC δ (by 5 μM rottlerin) partially suppressed the effect by E2. Application of 10 μM LIMKi (Ross-Macdonald et al., 2008), an inhibitor of LIMK, also prevented the effect by E2.

Since the concentrations of inhibitors are added to their recommended concentrations, the inhibitory effects cannot be non-specific due to the excess amount of inhibitors. It should be noted that these kinase inhibitors alone did not significantly affect the total spine density within experimental error, indicating that the observed inhibitory effects are not due to simple blockers' effects (Fig. 3B).

2.4.2. Spine head diameter analysis

Since observing the total spine density does not tell us enough for understanding the complex kinase effects, the changes in spine head diameter distribution were analyzed.

Blocking PI3K, Erk MAPK, p38 MAPK, and PKA abolished the effect by E2 on the dendritic spine densities, decreasing the density of the small-head spines, while significant change was not observed in middle- and large-head spines (Fig. 3C and D). Inhibiting all the PKC subfamilies significantly decreased the density of small-head spines without changes in middle- and large-head spines (Fig. 3C and D). Selective inhibition of PKC δ partially decreased small-head spines. Blocking LIMK decreased small- and large-head spines (Fig. 3C and D).

Fig. 3 – Effects of kinase blockers on E2-induced spine increase and change in morphology. Spines were analyzed along the secondary dendrites of pyramidal neurons in the stratum radiatum of CA1 neurons. (A) Maximal intensity projections onto XY plane from z-series confocal micrographs, showing spines along the dendrites of hippocampal CA1 pyramidal neurons. Dendrites without drug-treatments (Control), dendrites after E2-treatment for 2 h (E2). Bar, 5 μm . Images analyzed by Spiso-3D (S) and 3 dimensional model illustration (Model) are also shown. (B) (Left) Effect of treatments by E2 and kinase blockers on the total spine density. (Right) No effects by only blockers. Vertical axis is the average number of spines per 1 μm . A 2 h treatment in ACSF without drugs (Control), with 1 nM E2 (E2), with 1 nM E2 and 1 μM ICI 182,780 (E2+ICI) with 1 nM E2 and 10 μM LY294002 (PI3K inhibitor) (E2+LY), with 1 nM E2 and 25 μM U0126 (Erk MAPK inhibitor) (E2+U), with 1 nM E2 and 10 μM SB203580 (p38 MAPK inhibitor) (E2+SB), with 1 nM E2 and 10 μM H-89 (PKA inhibitor) (E2+H89), and with 1 nM E2 and 10 μM chelerythrine (PKC inhibitor) (E2+Chel), and with 1 nM E2 and 10 μM LIMKi (LIMK inhibitor) (E2+LIMKi). (C) Histogram of spine head diameters. Abbreviations are same as in (B). Vertical axis is the number of spines per 1 μm of dendrite. A 2 h treatment in ACSF without drugs (Control, dashed line), with E2 (black line), with E2+LY (red line), with E2+U (blue line), with E2+SB (green line), with E2+H89 (purple line), with E2+Chel (pink line), and with E2+LIMKi (yellow line). (D) Density of three subtypes of spines. Abbreviations are same as in (B). Vertical axis is the average number of spines per 1 μm of dendrite. From left to right, small-head spines (small), middle-head spines (middle), and large-head spines (large) type. In each group, control (open column), E2 (black column), E2+LY (red column), E2+U (blue column), E2+SB (green column), E2+H89 (purple column), E2+Chel (pink column), and E2+LIMKi (yellow column). (E) Representative spine images of confocal micrographs used for (B)–(D): E2 plus LY treatment (E2+LY); E2 plus U0126 treatment (E2+U); E2 plus SB treatment (E2+SB); E2 plus H-89 treatment (E2+H89); E2 plus chelerythrine treatment (E2+Chel), E2 plus LIMKi treatment (E2+LIMKi). Maximal intensity projection onto XY plane from z-series (MAX-XY), image analyzed by Spiso-3D (S) and 3 dimensional model (Model) are shown together. Bar, 5 μm . In (B)–(D), data are represented as mean \pm SEM. Statistical significance was defined as * $p < 0.05$, ** $p < 0.01$ vs E2 sample. For each drug treatment, we investigated 3 rats, 7 slices, 14 neurons, 28 dendrites and 1400–2000 spines. For control, we used 5 rats, 8 slices, 16 neurons, 31 dendrites and approx. 1700 spines.

2.5. Signaling pathways depending on other kinases and phosphatase (JNK, calcineurin, CaMKII, GSK3 β)

Blocking JNK, showed no change the total spine density, nor the subpopulations of spines (Fig. 4). The spine increase effect by E2 was blocked by cyclosporin A (1 μ M), an inhibitor of calcineurin, by KN-93 (1 μ M), an inhibitor of CaMKII, and by I8 (1 μ M), an inhibitor of GSK3 β . (Fig. 4). These kinase inhibitors alone did not significantly affect the total spine density within experimental error, indicating that the observed inhibitory effects are not due to simple blockers' effects (Fig. 4).

3. Discussion

3.1. Kinase involvement in E2-LTP upon weak-TBS

The current study demonstrates molecular mechanisms of rapid E2-induced LTP upon weak-TBS (sub-threshold stimulation) in adult hippocampus (Figs. 1 and 2). Induction of LTP upon weak-TBS by the presence of neurotrophic factors, including E2

and BDNF is observed for young 2–3 week-old rat hippocampus (Lynch et al., 2007; Kramar et al., 2009), however, the molecular mechanism of these LTP inductions had not been well understood. These neurotrophic factors fail to further increase full-LTP, which is induced upon strong stimulation, including tetanus stimulation (typically 100 Hz, 1 s) and full-TBS (Ooishi et al., 2012b), probably because these strong stimulations elevate EPSP to a saturated level which cannot be further enhanced by neurotrophic factors.

The current rapid action of E2 should be driven through kinases, including Erk MAPK, PKA and PKC, since their inhibitors completely suppressed E2-LTP by co-incubation with E2 for 30 min. Since Erk MAPK (together with ER α) is localized in the PSD fraction (Mukai et al., 2007, 2010; Hojo et al., 2008), the activation of Erk MAPK probably occurs within the postsynapses. Application of E2 rapidly phosphorylates tyrosine 1472 of NR2B (Dominguez et al., 2007). Co-incubation of NR2B inhibitor Ro25-6981 with E2 suppressed the E2-LTP (Fig. 1). Perfusion of CaMKII inhibitor KN-93 suppressed the E2-induced LTP during weak-TBS. We therefore hypothesize that the signaling pathway could be as follows: E2 \rightarrow synaptic ER α or ER β \rightarrow activation of Erk MAPK,

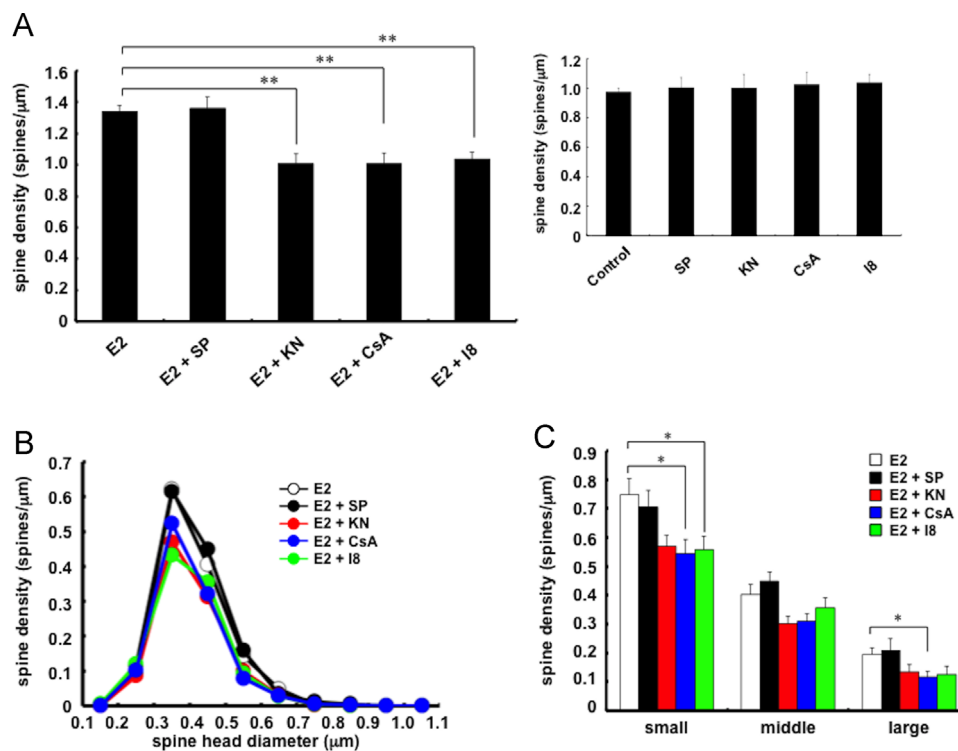


Fig. 4 – Effects of blockers of other kinases and phosphatase on E2-induced spinogenesis. (A) (Left) Effect of inhibitors on the presence of E2 on the total spine density in CA1 neurons. **(Right)** No effects by only inhibitors. Vertical axis is the average number of spines per 1 μ m. A 2 h treatment in ACSF without drugs (Control), with 1 nM E2 (E2), with 1 nM E2 and 10 μ M SP600125 (JNK inhibitor) (E2+SP), with 1 nM E2 and 1 μ M KN-93 (CaMKII inhibitor) (E2+KN), with 1 nM E2 and 1 μ M cyclosporin A (calcineurin inhibitor) (E2+CsA), and with 1 nM E2 and 1 μ M I8 (GSK3 β inhibitor) (E2+I8). **(B)** Histogram of spine head diameters. Abbreviations are same as in (A). Vertical axis is the number of spines per 1 μ m of dendrite. A 2 h treatment in ACSF with E2 (dashed line), with E2+SP (black line), with E2+KN (red line), with E2+CsA (blue line), and with E2+I8 (green line). **(C)** Density of three subtypes of spines. Abbreviations are same as in (A). Vertical axis is the average number of spines per 1 μ m of dendrite. From left to right, small-head spines (small), middle-head spines (middle), and large-head spines (large) type. In each group, E2 (open column), E2+SP (black column), E2+KN (red column), E2+CsA (blue column), and E2+I8 (green column). In (B) and (C), data are represented as mean \pm SEM. Statistical significance was defined as * p < 0.05, ** p < 0.01 vs E2 sample. For each drug treatment, we investigated 3 rats, 7 slices, 14 neurons, 28 dendrites and 1400–2000 spines.

PKC and PKA → activation of NMDA receptor by phosphorylation of NR2B → increase of Ca^{2+} influx through NMDA receptors during weak-TBS → activation of CaMKII → phosphorylation of AMPA receptors → enhancement of the magnitude of LTP (Fig. S4). This hypothetical signal sequence is also supported by earlier studies. Erk MAPK activation/phosphorylation by E2 is shown in neonatal mouse cortex (Toran-Allerand et al., 2002) and early adolescent rat hippocampus (Kim et al., 2002). The contribution of NR2B modulation by E2 to LTP induction is supported by genomic effects. Subcutaneous 2-time injections of E2 to ovariectomized female rats with interval of 24 h genomically enhance NR2B-derived EPSC at CA1 synapses after 24–48 h of the second injection, resulting in the increase of LTP (Smith and McMahon, 2006).

Involvement of mGluR1 in E2 signaling (E2 binding to ER α -mGluR1 complex induced CREB phosphorylation through Erk MAPK) has been shown in female hippocampal primary cultured neurons, but not in male neurons (Boulware et al., 2005, Boulware and Mermelstein, 2009). No involvement of mGluR1 in adult male E2 signaling was also observed in E2-LTP (Fig. 1B). Future investigations about mGluR1 in male and female E2 signaling might be useful to find possible hippocampal sex-differences.

3.2. Difference in E2 effects between matured and developing neural circuits

For series of electrophysiological experiments, Kawato's group have usually used 3 month-old adult rat hippocampus that has matured completed synaptic contacts in neural circuits. Importantly, E2 effects are often different between developing and matured neural circuits of the hippocampus. For example perfusion of only E2 does not affect baseline EPSP in 12 week-old (3 month-old) adult Wistar rats (Ito et al., 1999; Ogiue-Ikeda et al., 2008; Ooishi et al., 2012b); but perfusion of only E2 rapidly increases baseline EPSP in 4–6 week-old or 200–350 g (approx. 6–8 week-old) Sprague-Dauley rats (Foy et al., 1999; Bi et al., 2000; Kramar et al., 2009). Therefore, these differences about E2-induced elevation of baseline EPSP may depend on the age (12 weeks old or 4–8 weeks old) or strain (Wistar or Sprague-Dauley) of rats. Concerning 4 week-old male Wistar rats, we sometimes (less than 20% possibility) observed the rapid baseline EPSP elevation upon estradiol alone perfusion (Kawato, 2004; Mukai et al., 2006; Ogiue-Ikeda et al., 2008). On the other hand, concerning 12 week-old male Wistar rats, Ito's group demonstrates no rapid baseline elevation upon only E2 perfusion, as well as no enhancement of LTP (Ito et al., 1999). Interestingly, Foy and Thompson's group shows no rapid basal EPSP elevation (<3% elevation) upon estradiol alone perfusion in case of 3–5 month-old as well as 18–24 month-old Sprague-Dauley rats (Vouimba et al., 2000). Therefore, estradiol only may have the significant effect of rapid baseline elevation of synaptic transmission on younger rats (4–8 weeks old) and may not have the effect on older adult rats (12 weeks old or elder).

3.3. Difference and similarity in synaptic effects between androgen and estrogen

In the current study, the application of 10 nM DHT (but not 3 nM DHT) prevented 10 nM E2-induced LTP in adult hippocampal CA1. The signaling pathway might be “DHT → AR →

calcineurin → suppression of NMDA receptors → suppression of E2-LTP” (Fig. S4). Here, we consider the fact that calcineurin is known to desensitize the NMDA receptor subunit NR2A through dephosphorylation of a serine residue (Krupp et al., 2002), and that calcineurin inhibitor CsA blocked DHT-induced suppression of E2-LTP (Fig. 2B2).

Grassi, Pettorossi and co-workers showed that under blocking of ER by ICI, an additional inhibition of AR by flutamide induced moderate LTP (upon repetitive tetanus stimulation of 4 sets of 100 Hz, 1 s) in the developing CA1 hippocampal slices from postnatal 2–3 weeks-old rats (Pettorossi et al., 2013). This means that AR may have suppressive effects on LTP. Only AR antagonist, however, does not suppress LTP upon repetitive tetanus stimulation (Pettorossi et al., 2013). Suppressive effects by DHT on LTP are also suggested for CA3 mossy fiber. LTP of mossy fiber (upon 25 Hz, 1 s train, twice with a 10 s interval) is induced in hippocampal slices prepared from androgen-depleted (castrated) rats, whereas LTP is not induced in slices from control rats (Skucas et al., 2013). Administration of 50 nM DHT to androgen-depleted slices suppressed LTP (Skucas et al., 2013). Taken together, DHT and AR might prevent E2-induced hyperexcitability of CA1 synapses.

Androgen effects were very different on spinogenesis (new spine formation), compared with LTP (at pre-formed synapse). Similar to E2, DHT increased spine density (Hatanaka et al., in this Special Issue). DHT did not block E2-induced spine increase, when both DHT and E2 were applied. E2 plus DHT did not have additive effects on the spine increase, and DHT did not change E2-effects on spinogenesis.

3.4. Rapid effect of E2 on spine density and morphology (Kinase-mediated signaling model)

The current results of kinase inhibition suggest that the rapid effects of E2 were mediated by serine/threonine kinases, including PI3K, Erk MAPK, p38 MAPK, PKA, and PKC (Fig. 3) (Fig. S4). Because both ER and these kinases are present in spines, an efficient coupling between these proteins could occur at postsynapses (Milner et al., 2005; Mukai et al., 2007; Hojo et al., 2008).

In CA1 region, MAPK cascade may couple with PKA and PKC through PKC → Raf1 → MAPK, PKA → B-Raf → MAPK in synaptic modulation including LTP (Roberson et al., 1999). Take the knowledge into account, PKA, PKC and MAPK may be key kinases responsible for modulation of spines.

PI3K may also contribute to E2-induced spinogenesis. PI3K is the downstream signaling molecule of ER α , which promotes neuroprotection by phosphorylation of Akt (Garcia-Segura, 2007). E2 protects neuronal cell death through PI3K/Akt pathway, in the hippocampus upon ischemia (Yang et al., 2010), and in retina upon light-induced apoptosis (Mo et al., 2013).

Erk MAPK is known to phosphorylate cortactin, a structural protein associated to actin (MacQueen et al., 2003). Cortactin interacts with both F-actin and actin-related protein (Arp) 2/3 complex as well as scaffold protein Shank in the PSD at the SH3 domain (Weed et al., 1998; Campbell et al., 1999), resulting in promotion of actin fiber remodeling within spines. As a good example, upon BDNF stimulation, MAPK phosphorylates cortactin through interacting C-terminal of SH3 domain, resulting

in a reorganization of spine morphology (Iki et al., 2005). It is thus possible that E2 exerts its effect on spines through cortactin–actin pathway. Cortactin has multiple phosphorylation sites, including Ser⁴⁰⁵ and Ser⁴¹⁸, which are activated by MAPK (Campbell et al., 1999). Phosphorylation of cortactin may promote assembly of actin cytoskeletal matrices, resulting in spine formation or modulation of spine head (Hering and Sheng, 2003). These sites, including Ser¹¹³, are putative phosphorylation sites also for other serine/threonine kinase (PKA or PKC) that are activated by E2.

Besides cortactin, cofilin and LIMK are also good candidates for E2-induced actin reassembly, leading to spinogenesis (Clancy et al., 1992; Aizawa et al., 2001; Liston et al., 2013). It is known that corticosterone induces the phosphorylation of both LIMK and cofilin, leading to spinogenesis (Liston et al., 2013). Cofilin polymerizes actin filaments upon phosphorylation by LIMK (Clancy et al., 1992). PKC or RhoA may phosphorylate LIMK (Pilpel and Segal, 2004; Shi et al., 2009). LIMK may also be activated upon phosphorylation by p38 MAPK (Kobayashi et al., 2006).

Interestingly, the effect of E2 was completely blocked by inhibition of only one member of kinases, although many kinases participate in estrogen-induced spinogenesis (Fig. 3). These results suggest that E2-induced spine increase may need multiple phosphorylation of actin-modulating protein, including cortactin and cofilin.

3.5. Earlier studies about rapid ER action

We observed that ER is localized within spines and participates in rapid modulation effects of synapses and spines (Tsurugizawa et al., 2005; Mukai et al., 2007, 2010; Hojo et al., 2008).

E2 induces rapid CA1 spine increase through Erk MAPK (Mukai et al., 2007, 2010). E2 induces spine increase through PI3K pathway (Fig. 3). PI3K has some specific interactions with E2 signaling, for example, PI3K directly binds to estrogen receptor (Simoncini et al., 2000), and PI3K mediates E2-induced acute neuroprotection from apoptotic cell death by ischemia in hippocampal CA1 region (Jover-Mengual et al., 2010). E2 rapidly enhances NMDA-induced chemical-long term depression (LTD) in CA1 (Mukai et al., 2007, 2010).

Immunoelectron microscopic analysis demonstrates that ER α and ER β is localized not only in cytoplasm and nuclei but also inside of spines (Herrick et al., 2006; Mukai et al., 2007). These results support the idea that postsynaptic ER may mediate E2-induced rapid spinogenesis by activating several kinases.

3.6. Slow and genomic effects of E2

Concerning LTP study, subcutaneous 2-time injections of E2 to OVX female rats with interval of 24 h genomically enhance NR2B-derived EPSC at CA1 synapses after 24–48 h of the second injection (Snyder et al., 2011; Smith et al., 2002), resulting in the increase of LTP (Smith et al., 2002). Many *in vivo* dendritic spine analysis show the involvement of gonadal E2 in the cyclic change in the spine density across the estrous cycle (Gould et al., 1990; Woolley and McEwen, 1992; Kato et al., 2013), and the effect of E2 supplementation on the recovery of the spine density of CA1 neurons of OVX

female rats (Woolley and McEwen, 1993). In OVX rats, circulating E2 is undetectable and the spine density decreases significantly. These recovery effects of E2 (10 μ g/d, s.c.) took 2 days to be appeared (Woolley and McEwen, 1993).

It should be noted that the mechanisms of E2 action may be different between *in vivo* and *in vitro* experiments, because indirect effects of E2 may also occur *in vivo* through cholinergic or serotonergic neurons, which express ER and project to the hippocampus, in addition to direct influence of E2 on glutamatergic neurons (Guerra-Araiza et al., 2003).

3.7. Estrogen levels in the male and female hippocampus

E2 in the hippocampus should play a key role for rapid action through synaptic ER as a modulator of synaptic plasticity. The concentration of endogenous E2, DHT and T is determined to be approx. 8 nM, 7 nM and 17 nM, respectively, in freshly isolated hippocampus, with some variation between individual rats, by mass-spectrometric analysis (Hojo et al., 2009; Okamoto et al., 2012). Interestingly, E2 level in the male hippocampus (\sim 8 nM) was higher than that in female (0.6–4.3 nM) (Kato et al., 2013). In addition to hippocampal synthesis of T, T may also reach the hippocampus via blood circulation (\sim 15 nM in plasma). After castration hippocampal T goes down to \sim 3 nM, while hippocampal E2 stays the same (\sim 8 nM) even after castration.

It should be noted that, in 'acute' slices (used for current analysis of synaptic plasticity), the levels of E2, DHT and T decreased to below 0.5 nM due to the slice recovery incubation with ACSF after fresh slice preparations (Hojo et al., 2009, 2011, Ooishi et al., 2012a, 2012b). In the current study, the exogenous application of 1–10 nM E2 was used to elevate the hippocampal androgen level from ACSF-washed level ('acute' slice) ($<$ 0.5 nM) back to the endogenous level rapidly (Ooishi et al., 2012b). Exogenous application of E2 was employed to modulate hippocampal estrogen levels, because until now the method of rapid elevation of endogenous estrogen concentration through activation of its synthesis pathway is not yet established. To investigate in a more intrinsic condition, the methods of rapid activation of endogenous synthesis of estrogen should be developed, such as NMDA-induced synthesis (Kawato et al., 2002, Hojo et al., 2004), or 1–10 Hz low frequency electric stimulation-induced synthesis.

Interestingly, E2 level in the female hippocampus (0.6–4.3 nM) was lower than that in male (\sim 8 nM). The high level of male hippocampal E2 (8 nM) may be, partly due to, conversion from circulating (high level) T (\sim 15 nM), penetrating into the hippocampus. The moderately high level of female hippocampal E2 (0.5–4.3 nM) may be mainly due to the conversion from circulating PROG (20–50 nM) in addition to hippocampus-synthesized PROG, since circulating E2, E1, T were too low ($<$ 1 nM) to contribute.

3.8. New perspectives of estrogen and androgen as central modulators

Estrogen and androgen should be recognized now as central (not peripheral) modulators of memory performance, with rapid synaptic regulation (Balthazart and Ball, 2006). Sex-steroids had been thought to be peripheral regulators of memory performance, with daily circadian rhythm or estrus cycle. This was due

to the absence of evidence that sex-steroids are synthesized within the adult brain, although steroid synthesis was indicated in neonatal brains (Kretz et al., 2004; Higo et al., 2009; Munetsuna et al., 2009; Konkle and McCarthy, 2011). This is because, for example, cytochrome P450 (17 α), dehydroepiandrosterone (DHEA) synthase, had long been not found in the adult brain, with neither mRNA nor protein analysis (Corpechot et al., 1981; Baulieu, 1997; Baulieu and Robel, 1998). After finding adult hippocampal/brain synthesis of estrogen and androgen from cholesterol (Kimoto et al., 2001; Kawato et al., 2002; Hojo et al., 2004), many experimental results have been accumulated, which favor their roles as local paracrine/intracrine regulators. However, still some controversy exists concerning observed sex-steroid levels in adult male and female brain (Beyer and Rune, 2012; Vierk et al., 2012), which might be partly due to some difficulties, in anatomical procedures (hippocampal tissues should be taken out within 30 min after decapitation), and in purification procedures of steroids (steroids should be extracted from the fresh brain, not from the brain stored being frozen). If we slowly take out hippocampal tissues, later than 1 h, after decapitation, we may lose some estrogen and androgen, which might be due to peroxidation of lipids and steroids. If we extract steroids from a frozen stored brain, we might lose some estrogen and androgen, which might be due to oxidation of steroids.

Local paracrine/intracrine regulation may consist of actions of synaptic/extranuclear receptors, which drive kinase/phosphatase signaling, different from slow signaling through gene transcription via classical nuclear steroid receptors. It should be noted that non-genomic types of rapid signaling might also trigger slow genomic action in the downstream, since kinases may move into the nuclei, resulting in gene transcription.

4. Experimental procedures

4.1. Animals

Young adult male Wistar rats (12 week old, 320–360 g) were purchased from Tokyo Experimental Animals Supply (Japan). All animals were maintained under a 12 h light/12 dark cycle and free access to food and water. The experimental procedure of this research was approved by the Committee for Animal Research of the University of Tokyo.

4.2. Chemicals

Lucifer Yellow was obtained from Molecular Probes (USA). Cyanonitroquinoxaline-dione (CNQX), MK-801, PD98059, SB203580, LY294002, cyclosporin A (CsA), cycloheximide (CHX), actinomycin D (actD), Ro25-6981 and *N*-methyl-D-aspartate (NMDA) were purchased from Sigma (USA). H-89, chelerythrine, rottlerin, LIMKi and KN-93 were from Calbiochem (USA). Estradiol, SP600125, U0126, HF, ICI182, 780 from Wako Pure Chemical Industries (Japan).

4.3. Slice preparation

Adult male rats were deeply anaesthetized and decapitated. Immediately after decapitation, the brain was removed from the skull and placed in ice-cold oxygenated (95% O₂, 5% CO₂) artificial cerebrospinal fluid (ACSF) containing (in mM): 124

NaCl, 5 KCl, 1.25 NaH₂PO₄, 2 MgSO₄, 2 CaCl₂, 22 NaHCO₃, and 10 D-glucose (all from Wako); pH was set at 7.4. The hippocampus was then dissected and 400 μ m thick transverse slices to the long axis, from the middle third of the hippocampus, were prepared with a vibratome (Dosaka, Japan). These slices were ‘fresh’ slices without ACSF incubation. Slices were then incubated in oxygenated ACSF for 2 h (slice recovery processes) in order to obtain widely used ‘acute slices’.

4.4. LTP measurements upon weak-TBS in the CA1 slices

The acute slice was incubated with E2 at 10 nM for another 0.5 h. The slice was then transferred to a recording chamber, interfaced and continuously perfused (2 ml/min) with oxygenated ACSF at 33 °C (Hasegawa et al., 2014).

Experimental details with custom multielectrode probes are described elsewhere (Mukai et al., 2007; Ogiue-Ikeda et al., 2008). Briefly, slices were positioned on a custom multielectrode probe in which 64 planar microelectrodes (Alpha MED Scientific, Japan) were particularly designated to densely cover the important regions containing essential synaptic contacts of pyramidal neurons of the stratum radiatum in CA1. EPSP responses were measured with selected electrodes in CA1. We determined the input–output curve of EPSP by gradually increasing the stimulus intensity. The interval of the stimulation was 45 s. When responses were saturated, we calculated the stimulus intensity which gave the half maximum of EPSP.

For investigation of E2-inducible LTP, the weak-TBS was applied to the Schaffer collaterals. Typically the “weak-TBS” stimuli were delivered as discrete 3 bursts separated by 200 ms (Kramar et al., 2009). One burst consists of 5 pulses at 100 Hz. The “full-TBS” consists of 10 bursts (total 50 pulses). Although the weak-TBS induced sub-threshold LTP in the absence of E2, the weak-TBS induced full-LTP.

For induction of paired-pulse facilitation (PPF), paired pulse stimulation was applied to the Schaffer collaterals. The interval between these stimuli was 50 ms.

4.5. Imaging and analysis of dendritic spine density and morphology

4.5.1. Hippocampal slice preparation and current injection of Lucifer yellow

Male rats aged 12 weeks were deeply anesthetized and decapitated. The same ‘acute’ slices used for LTP experiments were used for spinogenesis. These ‘acute’ slices (used worldwide) were then incubated with 1–10 nM E2 together with inhibitors of protein kinases, ion channels, or protein synthesis. Slices were then fixed with 4% paraformaldehyde in PBS at 4 °C overnight. Neurons within slices were visualized by an injection of Lucifer Yellow (Molecular Probes, USA) under Nikon E600FN microscope (Japan) equipped with a C2400-79H infrared camera (Hamamatsu Photonics, Japan) and with a 40 \times water immersion lens (Nikon, Japan).

Current injection was performed with glass electrode filled with 5% Lucifer Yellow for 15 min, using Axopatch 200B (Axon Instruments, USA). Approximately five neurons within a depth

of 100–200 μm from the surface of a slice were injected with Lucifer Yellow (Duan et al., 2002).

4.5.2. Confocal laser microscopy and morphological analysis
The imaging was performed from sequential z-series scans with confocal laser scan microscope (LSM5; Carl Zeiss, Germany) at high zoom ($\times 3.0$) with a $63\times$ water immersion lens, NA 1.2. For Lucifer Yellow, the excitation and emission wavelengths were 488 nm and 515 nm, respectively. For analysis of spines, three-dimensional image was reconstructed from approximately 40 sequential z-series sections of every 0.45 μm with a $63\times$ water immersion lens, NA 1.2. The applied zoom factor ($\times 3.0$) yielded 23 pixels per 1 μm . The z-axis resolution was approximately 0.71 μm . The confocal lateral resolution was approximately 0.26 μm . Our resolution limits were regarded to be sufficient to allow the determination of the density of spines. Confocal images were then deconvoluted using AutoDeblur software (AutoQuant, USA).

The density of spines as well as the head diameter was analyzed with Spiso-3D (automated software mathematically calculating geometrical parameters of spines) developed by Bioinformatics Project of Kawato's group (Mukai et al., 2011). Spiso-3D has an equivalent capacity with NeuroLucida (MicroBrightField, USA), furthermore, Spiso-3D considerably reduces human errors and experimenter labor. The single apical dendrite was analyzed separately. The spine density was calculated from the number of spines along secondary dendrites having a total length of 40–70 μm . These dendrites were present within the stratum radiatum, between 100 and 200 μm from the soma. Spine shapes were classified into three categories as follows. (1) A small-head spine, whose head diameter is smaller than 0.4 μm . (2) A middle-head spine, which has 0.4–0.5 μm spine head. (3) A large-head spine, whose head diameter is larger than 0.5 μm . These three categories were useful to distinguish different responses upon kinase inhibitor application. Because the majority of spines (>95%) had a distinct head and neck, and stubby spines and filopodium did not contribute much to overall changes, we analyzed spines having a distinct head.

4.6. Statistical analysis

For E2-LTP analysis, we defined the LTP ratio as the average of EPSP slope level for $t=50$ –60 min. One-way ANOVA, followed by a Tukey and Kramer's post hoc test were used for multiple comparisons between drug treatments of LTP experiments. For DHT-induced suppression of E2-LTP analysis, three-way ANOVA was used for multiple comparisons between drug treatments.

For spine analysis, the significance of E2 and drug effects were first examined by one-way ANOVA (analysis of variance), followed by Tukey–Kramer post-hoc multiple comparisons test.

Acknowledgments

We thank Tom Shindo for the technical assistance.

Appendix A. Supporting information

Supplementary data associated with this article can be available in the online version at <http://dx.doi.org/10.1016/j.brainres.2014.12.056>.

REFERENCES

- Aizawa, H., Wakatsuki, S., Ishii, A., Moriyama, K., Sasaki, Y., Ohashi, K., Sekine-Aizawa, Y., Sehara-Fujisawa, A., Mizuno, K., Goshima, Y., Yahara, I., 2001. Phosphorylation of cofilin by LIM-kinase is necessary for semaphorin 3A-induced growth cone collapse. *Nat. Neurosci.* 4, 367–373.
- Balthazart, J., Ball, G.F., 2006. Is brain estradiol a hormone or a neurotransmitter?. *Trends Neurosci.* 29, 241–249.
- Baulieu, E.E., 1997. Neurosteroids: of the nervous system, by the nervous system, for the nervous system. *Recent Prog. Horm. Res.* 52, 1–32.
- Baulieu, E.E., Robel, P., 1998. Dehydroepiandrosterone (DHEA) and dehydroepiandrosterone sulfate (DHEAS) as neuroactive neurosteroids. *Proc. Natl. Acad. Sci. U.S.A.* 95, 4089–4091.
- Beyer, C., Rune, G., 2012. Steroids in the brain: regulators of brain plasticity and protectors against neuronal damage. *J. Steroid Biochem. Mol. Biol.* 131, 1.
- Bi, R., Broutman, G., Foy, M.R., Thompson, R.F., Baudry, M., 2000. The tyrosine kinase and mitogen-activated protein kinase pathways mediate multiple effects of estrogen in hippocampus. *Proc. Natl. Acad. Sci. U.S.A.* 97, 3602–3607.
- Boulware, M.I., Mermelstein, P.G., 2009. Membrane estrogen receptors activate metabotropic glutamate receptors to influence nervous system physiology. *Steroids* 74, 608–613.
- Boulware, M.I., Weick, J.P., Becklund, B.R., Kuo, S.P., Groth, R.D., Mermelstein, P.G., 2005. Estradiol activates group I and II metabotropic glutamate receptor signaling, leading to opposing influences on cAMP response element-binding protein. *J. Neurosci.* 25, 5066–5078.
- Campbell, D.H., Sutherland, R.L., Daly, R.J., 1999. Signaling pathways and structural domains required for phosphorylation of EMS1/cortactin. *Cancer Res.* 59, 5376–5385.
- Chijiwa, T., Mishima, A., Hagiwara, M., Sano, M., Hayashi, K., Inoue, T., Naito, K., Toshioka, T., Hidaka, H., 1990. Inhibition of forskolin-induced neurite outgrowth and protein phosphorylation by a newly synthesized selective inhibitor of cyclic AMP-dependent protein kinase, N-[2-(p-bromocinnamylamino)ethyl]-5-isoquinolinesulfonamide (H-89), of PC12D pheochromocytoma cells. *J. Biol. Chem.* 265, 5267–5272.
- Clancy, A.N., Bonsall, R.W., Michael, R.P., 1992. Immunohistochemical labeling of androgen receptors in the brain of rat and monkey. *Life Sci.* 50, 409–417.
- Corpechot, C., Robel, P., Axelson, M., Sjøvall, J., Baulieu, E.E., 1981. Characterization and measurement of dehydroepiandrosterone sulfate in rat brain. *Proc. Natl. Acad. Sci. U.S.A.* 78, 4704–4707.
- Dominguez, R., Liu, R., Baudry, M., 2007. 17-Beta-estradiol-mediated activation of extracellular-signal regulated kinase, phosphatidylinositol 3-kinase/protein kinase B-Akt and N-methyl-D-aspartate receptor phosphorylation in cortical synaptoneuroosomes. *J. Neurochem.* 101, 232–240.
- Duan, H., Wearne, S.L., Morrison, J.H., Hof, P.R., 2002. Quantitative analysis of the dendritic morphology of corticocortical projection neurons in the macaque monkey association cortex. *Neuroscience* 114, 349–359.

- Ehrlich, I., Malinow, R., 2004. Postsynaptic density 95 controls AMPA receptor incorporation during long-term potentiation and experience-driven synaptic plasticity. *J. Neurosci.* 24, 916–927.
- Favata, M.F., Horiuchi, K.Y., Manos, E.J., Daulerio, A.J., Stradley, D.A., Feeser, W.S., Van Dyk, D.E., Pitts, W.J., Earl, R.A., Hobbs, F., Copeland, R.A., Magolda, R.L., Scherle, P.A., Trzaskos, J.M., 1998. Identification of a novel inhibitor of mitogen-activated protein kinase. *J. Biol. Chem.* 273, 18623–18632.
- Fischer, G., Mutel, V., Trube, G., Malherbe, P., Kew, J.N., Mohacsi, E., Heitz, M.P., Kemp, J.A., 1997. Ro 25-6981, a highly potent and selective blocker of N-methyl-D-aspartate receptors containing the NR2B subunit. Characterization in vitro. *J. Pharmacol. Exp. Ther.* 283, 1285–1292.
- Foy, M.R., Xu, J., Xie, X., Brinton, R.D., Thompson, R.F., Berger, T.W., 1999. 17Beta-estradiol enhances NMDA receptor-mediated EPSPs and long-term potentiation. *J. Neurophysiol.* 81, 925–929.
- Garcia-Segura, L.M., Diz-Chaves, Y., Perez-Martin, M., Darnaudery, M., 2007. Estradiol, insulin-like growth factor-I and brain aging. *Psychoneuroendocrinology* 32 (1), S57–S61.
- Gould, E., Woolley, C.S., Frankfurt, M., McEwen, B.S., 1990. Gonadal steroids regulate dendritic spine density in hippocampal pyramidal cells in adulthood. *J. Neurosci.* 10, 1286–1291.
- Gu, Q., Korach, K.S., Moss, R.L., 1999. Rapid action of 17beta-estradiol on kainate-induced currents in hippocampal neurons lacking intracellular estrogen receptors. *Endocrinology* 140, 660–666.
- Gu, Q., Moss, R.L., 1996. 17 Beta-estradiol potentiates kainate-induced currents via activation of the cAMP cascade. *J. Neurosci.* 16, 3620–3629.
- Guerra-Araiza, C., Villamar-Cruz, O., Gonzalez-Arenas, A., Chavira, R., Camacho-Arroyo, I., 2003. Changes in progesterone receptor isoforms content in the rat brain during the oestrous cycle and after oestradiol and progesterone treatments. *J. Neuroendocrinol.* 15, 984–990.
- Hasegawa, Y., Mukai, H., Asashima, M., Hojo, Y., Ikeda, M., Komatsuzaki, Y., Ooishi, Y., Kawato, S., 2014. Acute modulation of synaptic plasticity of pyramidal neurons by activin in adult hippocampus. *Front. Neural. Circuits* 8, 56.
- Herbert, J.M., Augereau, J.M., Gleye, J., Maffrand, J.P., 1990. Chelerythrine is a potent and specific inhibitor of protein kinase C. *Biochem. Biophys. Res. Commun.* 172, 993–999.
- Hering, H., Sheng, M., 2003. Activity-dependent redistribution and essential role of cortactin in dendritic spine morphogenesis. *J. Neurosci.* 23, 11759–11769.
- Herrick, S.P., Waters, E.M., Drake, C.T., McEwen, B.S., Milner, T.A., 2006. Extranuclear estrogen receptor beta immunoreactivity is on doublecortin-containing cells in the adult and neonatal rat dentate gyrus. *Brain Res.* 1121, 46–58.
- Hojo, S., Hojo, Y., Ishii, H., Kominami, T., Nakajima, K., Poirier, D., Kimoto, T., Kawato, S., 2009. Comparison of sex-steroid synthesis between neonatal and adult rat hippocampus. *Biochem. Biophys. Res. Commun.* 385, 62–66.
- Hojo, Y., Hattori, T.A., Enami, T., Furukawa, A., Suzuki, K., Ishii, H.T., Mukai, H., Morrison, J.H., Janssen, W.G., Kominami, S., Harada, N., Kimoto, T., Kawato, S., 2004. Adult male rat hippocampus synthesizes estradiol from pregnenolone by cytochromes P45017alpha and P450 aromatase localized in neurons. *Proc. Natl. Acad. Sci. U.S.A.* 101, 865–870.
- Hojo, Y., Higo, S., Ishii, H., Ooishi, Y., Mukai, H., Murakami, G., Kominami, T., Kimoto, T., Honma, S., Poirier, D., Kawato, S., 2009. Comparison between hippocampus-synthesized and circulation-derived sex steroids in the hippocampus. *Endocrinology* 150, 5106–5112.
- Hojo, Y., Higo, S., Kawato, S., Hatanaka, Y., Ooishi, Y., Murakami, G., Ishii, H., Komatsuzaki, Y., Ogiue-Ikeda, M., Mukai, H., Kimoto, T., 2011. Hippocampal synthesis of sex steroids and corticosteroids: essential for modulation of synaptic plasticity. *Front. Endocrinol. (Lausanne)* 2, 43.
- Hojo, Y., Murakami, G., Mukai, H., Higo, S., Hatanaka, Y., Ogiue-Ikeda, M., Ishii, H., Kimoto, T., Kawato, S., 2008. Estrogen synthesis in the brain—role in synaptic plasticity and memory. *Mol. Cell Endocrinol.* 290, 31–43.
- Iki, J., Inoue, A., Bito, H., Okabe, S., 2005. Bi-directional regulation of postsynaptic cortactin distribution by BDNF and NMDA receptor activity. *Eur. J. Neurosci.* 22, 2985–2994.
- Ito, K., Skinkle, K.L., Hicks, T.P., 1999. Age-dependent, steroid-specific effects of oestrogen on long-term potentiation in rat hippocampal slices. *J. Physiol.* 515, 209–220 (Pt 1).
- Jover-Mengual, T., Miyawaki, T., Latuszek, A., Alborch, E., Zukin, R.S., Etgen, A.M., 2010. Acute estradiol protects CA1 neurons from ischemia-induced apoptotic cell death via the PI3K/Akt pathway. *Brain Res.* 1321, 1–12.
- Kato, A., Hojo, Y., Higo, S., Komatsuzaki, Y., Murakami, G., Yoshino, H., Uebayashi, M., Kawato, S., 2013. Female hippocampal estrogens have a significant correlation with cyclic fluctuation of hippocampal spines. *Front. Neural. Circuits* 7, 149.
- Kawato, S., 2004. Endocrine disrupters as disrupters of brain function: a neurosteroid viewpoint. *Environ. Sci.* 11, 1–14.
- Kawato, S., Hojo, Y., Kimoto, T., 2002. Histological and metabolism analysis of P450 expression in the brain. *Methods Enzymol.* 357, 241–249.
- Kawato, S., Yamada, M., Kimoto, T., 2003. Brain neurosteroids are 4th generation neuromessengers in the brain: cell biophysical analysis of steroid signal transduction. *Adv. Biophys.* 37, 1–48.
- Kim, J.S., Kim, H.Y., Kim, J.H., Shin, H.K., Lee, S.H., Lee, Y.S., Son, H., 2002. Enhancement of rat hippocampal long-term potentiation by 17 beta-estradiol involves mitogen-activated protein kinase-dependent and -independent components. *Neurosci. Lett.* 332, 65–69.
- Kimoto, T., Tsurugizawa, T., Ohta, Y., Makino, J., Tamura, H., Hojo, Y., Takata, N., Kawato, S., 2001. Neurosteroid synthesis by cytochrome p450-containing systems localized in the rat brain hippocampal neurons: N-methyl-D-aspartate and calcium-dependent synthesis. *Endocrinology* 142, 3578–3589.
- Kobayashi, M., Nishita, M., Mishima, T., Ohashi, K., Mizuno, K., 2006. MAPKAPK-2-mediated LIM-kinase activation is critical for VEGF-induced actin remodeling and cell migration. *Embo J.* 25, 713–726.
- Konkle, A.T., McCarthy, M.M., 2011. Developmental time course of estradiol, testosterone, and dihydrotestosterone levels in discrete regions of male and female rat brain. *Endocrinology* 152, 223–235.
- Kramar, E.A., Chen, L.Y., Brandon, N.J., Rex, C.S., Liu, F., Gall, C.M., Lynch, G., 2009. Cytoskeletal changes underlie estrogen's acute effects on synaptic transmission and plasticity. *J. Neurosci.* 29, 12982–12993.
- Kretz, O., Fester, L., Wehrenberg, U., Zhou, L., Brauckmann, S., Zhao, S., Prange-Kiel, J., Naumann, T., Jarry, H., Frotscher, M., Rune, G.M., 2004. Hippocampal synapses depend on hippocampal estrogen synthesis. *J. Neurosci.* 24, 5913–5921.
- Krupp, J.J., Vissel, B., Thomas, C.G., Heinemann, S.F., Westbrook, G.L., 2002. Calcineurin acts via the C-terminus of NR2A to modulate desensitization of NMDA receptors. *Neuropharmacology* 42, 593–602.
- Leranth, C., Shanabrough, M., Horvath, T.L., 2000. Hormonal regulation of hippocampal spine synapse density involves subcortical mediation. *Neuroscience* 101, 349–356.
- Leranth, C., Shanabrough, M., Redmond Jr., D.E., 2002. Gonadal hormones are responsible for maintaining the integrity of spine synapses in the CA1 hippocampal subfield of female nonhuman primates. *J. Comp. Neurol.* 447, 34–42.
- Liston, C., Cichon, J.M., Jeanneteau, F., Jia, Z., Chao, M.V., Gan, W.B., 2013. Circadian glucocorticoid oscillations promote learning-

- dependent synapse formation and maintenance. *Nat. Neurosci.* 16, 698–705.
- Lynch, G., Kramar, E.A., Rex, C.S., Jia, Y., Chappas, D., Gall, C.M., Simmons, D.A., 2007. Brain-derived neurotrophic factor restores synaptic plasticity in a knock-in mouse model of Huntington's disease. *J. Neurosci.* 27, 4424–4434.
- MacQueen, G.M., Campbell, S., McEwen, B.S., Macdonald, K., Amano, S., Joffe, R.T., Nahmias, C., Young, L.T., 2003. Course of illness, hippocampal function, and hippocampal volume in major depression. *Proc. Natl. Acad. Sci. U.S.A.* 100, 1387–1392.
- McEwen, B.S., Alves, S.E., 1999. Estrogen actions in the central nervous system. *Endocr. Rev.* 20, 279–307.
- Milner, T.A., Ayoola, K., Drake, C.T., Herrick, S.P., Tabori, N.E., McEwen, B.S., Warriar, S., Alves, S.E., 2005. Ultrastructural localization of estrogen receptor beta immunoreactivity in the rat hippocampal formation. *J. Comp. Neurol.* 491, 81–95.
- Mo, M.S., Li, H.B., Wang, B.Y., Wang, S.L., Zhu, Z.L., Yu, X.R., 2013. PI3K/Akt and NF-kappaB activation following intravitreal administration of 17beta-estradiol: neuroprotection of the rat retina from light-induced apoptosis. *Neuroscience* 228, 1–12.
- Mukai, H., Hatanaka, Y., Mitsuhashi, K., Hojo, Y., Komatsuzaki, Y., Sato, R., Murakami, G., Kimoto, T., Kawato, S., 2011. Automated analysis of spines from confocal laser microscopy images: application to the discrimination of androgen and estrogen effects on spinogenesis. *Cereb Cortex* 21, 2704–2711.
- Mukai, H., Kimoto, T., Hojo, Y., Kawato, S., Murakami, G., Higo, S., Hatanaka, Y., Ogiue-Ikeda, M., 2010. Modulation of synaptic plasticity by brain estrogen in the hippocampus. *Biochim. Biophys. Acta* 1800, 1030–1044.
- Mukai, H., Takata, N., Ishii, H.T., Tanabe, N., Hojo, Y., Furukawa, A., Kimoto, T., Kawato, S., 2006. Hippocampal synthesis of estrogens and androgens which are paracrine modulators of synaptic plasticity: synaptocrinology. *Neuroscience* 138, 757–764.
- Mukai, H., Tsurugizawa, T., Murakami, G., Kominami, S., Ishii, H., Ogiue-Ikeda, M., Takata, N., Tanabe, N., Furukawa, A., Hojo, Y., Ooishi, Y., Morrison, J.H., Janssen, W.G., Rose, J.A., Chambon, P., Kato, S., Izumi, S., Yamazaki, T., Kimoto, T., Kawato, S., 2007. Rapid modulation of long-term depression and spinogenesis via synaptic estrogen receptors in hippocampal principal neurons. *J. Neurochem.* 100, 950–967.
- Munetsuna, E., Hojo, Y., Hattori, M., Ishii, H., Kawato, S., Ishida, A., Kominami, S.A., Yamazaki, T., 2009. Retinoic acid stimulates 17beta-estradiol and testosterone synthesis in rat hippocampal slice cultures. *Endocrinology* 150, 4260–4269.
- Murphy, D.D., Segal, M., 1996. Regulation of dendritic spine density in cultured rat hippocampal neurons by steroid hormones. *J. Neurosci.* 16, 4059–4068.
- Nebieridze, N., Zhang, X.L., Chachua, T., Velisek, L., Stanton, P.K., Veliskova, J., 2012. Beta-estradiol unmasks metabotropic receptor-mediated metaplasticity of NMDA receptor transmission in the female rat dentate gyrus. *Psychoneuroendocrinology* 37, 1845–1854.
- Ogiue-Ikeda, M., Tanabe, N., Mukai, H., Hojo, Y., Murakami, G., Tsurugizawa, T., Takata, N., Kimoto, T., Kawato, S., 2008. Rapid modulation of synaptic plasticity by estrogens as well as endocrine disrupters in hippocampal neurons. *Brain Res. Rev.* 57, 363–375.
- Okamoto, M., Hojo, Y., Inoue, K., Matsui, T., Kawato, S., McEwen, B.S., Soya, H., 2012. Mild exercise increases dihydrotestosterone in hippocampus providing evidence for androgenic mediation of neurogenesis. *Proc. Natl. Acad. Sci. U.S.A.* 109, 13100–13105.
- Ooishi, Y., Kawato, S., Hojo, Y., Hatanaka, Y., Higo, S., Murakami, G., Komatsuzaki, Y., Ogiue-Ikeda, M., Kimoto, T., Mukai, H., 2012a. Modulation of synaptic plasticity in the hippocampus by hippocampus-derived estrogen and androgen. *J. Steroid Biochem. Mol. Biol.* 131, 37–51.
- Ooishi, Y., Mukai, H., Hojo, Y., Murakami, G., Hasegawa, Y., Shindo, T., Morrison, J.H., Kimoto, T., Kawato, S., 2012b. Estradiol rapidly rescues synaptic transmission from corticosterone-induced suppression via synaptic/extranuclear steroid receptors in the hippocampus. *Cereb. Cortex* 22, 926–936.
- Pettorossi, V.E., Di Mauro, M., Scarduzio, M., Panichi, R., Tozzi, A., Calabresi, P., Grassi, S., 2013. Modulatory role of androgenic and estrogenic neurosteroids in determining the direction of synaptic plasticity in the CA1 hippocampal region of male rats. *Physiol. Rep.* 1, e00185.
- Pilpel, Y., Segal, M., 2004. Activation of PKC induces rapid morphological plasticity in dendrites of hippocampal neurons via Rac and Rho-dependent mechanisms. *Eur. J. Neurosci.* 19, 3151–3164.
- Pozzo-Miller, L.D., Inoue, T., Murphy, D.D., 1999. Estradiol increases spine density and NMDA-dependent Ca²⁺ transients in spines of CA1 pyramidal neurons from hippocampal slices. *J. Neurophysiol.* 81, 1404–1411.
- Razandi, M., Pedram, A., Greene, G.L., Levin, E.R., 1999. Cell membrane and nuclear estrogen receptors (ERs) originate from a single transcript: studies of ERalpha and ERbeta expressed in Chinese hamster ovary cells. *Mol. Endocrinol.* 13, 307–319.
- Roberson, E.D., English, J.D., Adams, J.P., Selcher, J.C., Kondratieck, C., Sweatt, J.D., 1999. The mitogen-activated protein kinase cascade couples PKA and PKC to cAMP response element binding protein phosphorylation in area CA1 of hippocampus. *J. Neurosci.* 19, 4337–4348.
- Ross-Macdonald, P., de Silva, H., Guo, Q., Xiao, H., Hung, C.Y., Penhallow, B., Markwalder, J., He, L., Attar, R.M., Lin, T.A., Seitz, S., Tilford, C., Wardwell-Swanson, J., Jackson, D., 2008. Identification of a nonkinase target mediating cytotoxicity of novel kinase inhibitors. *Mol. Cancer Ther.* 7, 3490–3498.
- Shi, Y., Pontrello, C.G., DeFea, K.A., Reichardt, L.F., Ethell, I.M., 2009. Focal adhesion kinase acts downstream of EphB receptors to maintain mature dendritic spines by regulating cofilin activity. *J. Neurosci.* 29, 8129–8142.
- Shinohara, Y., Hirase, H., Watanabe, M., Itakura, M., Takahashi, M., Shigemoto, R., 2008. Left-right asymmetry of the hippocampal synapses with differential subunit allocation of glutamate receptors. *Proc. Natl. Acad. Sci. U.S.A.* 105, 19498–19503.
- Simoncini, T., Hafezi-Moghadam, A., Brazil, D.P., Ley, K., Chin, W.W., Liao, J.K., 2000. Interaction of oestrogen receptor with the regulatory subunit of phosphatidylinositol-3-OH kinase. *Nature* 407, 538–541.
- Skucas, V.A., Duffy, A.M., Harte-Hargrove, L.C., Magagna-Poveda, A., Radman, T., Chakraborty, G., Schroeder, C.E., MacLusky, N.J., Scharfman, H.E., 2013. Testosterone depletion in adult male rats increases mossy fiber transmission, LTP, and sprouting in area CA3 of hippocampus. *J. Neurosci.* 33, 2338–2355.
- Smith, C.C., McMahan, L.L., 2006. Estradiol-induced increase in the magnitude of long-term potentiation is prevented by blocking NR2B-containing receptors. *J. Neurosci.* 26, 8517–8522.
- Smith, M.D., Jones, L.S., Wilson, M.A., 2002. Sex differences in hippocampal slice excitability: role of testosterone. *Neuroscience* 109, 517–530.
- Snyder, M.A., Cooke, B.M., Woolley, C.S., 2011. Estradiol potentiation of NR2B-dependent EPSCs is not due to changes in NR2B protein expression or phosphorylation. *Hippocampus* 21, 398–408.
- Toran-Allerand, C.D., Guan, X., MacLusky, N.J., Horvath, T.L., Diano, S., Singh, M., Connolly Jr, E.S., Nethrapalli, I.S., Tinnikov, A.A., 2002. ER-X: a novel, plasma membrane-associated, putative estrogen receptor that is regulated during development and after ischemic brain injury. *J. Neurosci.* 22, 8391–8401.

- Tsurugizawa, T., Mukai, H., Tanabe, N., Murakami, G., Hojo, Y., Kominami, S., Mitsuhashi, K., Komatsuzaki, Y., Morrison, J.H., Janssen, W.G., Kimoto, T., Kawato, S., 2005. Estrogen induces rapid decrease in dendritic thorns of CA3 pyramidal neurons in adult male rat hippocampus. *Biochem. Biophys. Res. Commun.* 337, 1345–1352.
- Vierk, R., Glassmeier, G., Zhou, L., Brandt, N., Fester, L., Dudzinski, D., Wilkars, W., Bender, R.A., Lewerenz, M., Gloger, S., Graser, L., Schwarz, J., Rune, G.M., 2012. Aromatase inhibition abolishes LTP generation in female but not in male mice. *J. Neurosci.* 32, 8116–8126.
- Vouimba, R.M., Foy, M.R., Foy, J.G., Thompson, R.F., 2000. 17Beta-estradiol suppresses expression of long-term depression in aged rats. *Brain Res. Bull.* 53, 783–787.
- Weed, S.A., Du, Y., Parsons, J.T., 1998. Translocation of cortactin to the cell periphery is mediated by the small GTPase Rac1. *J. Cell Sci.* 111, 2433–2443 (Pt 16).
- Wiederrecht, G., Lam, E., Hung, S., Martin, M., Sigal, N., 1993. The mechanism of action of FK-506 and cyclosporin A. *Ann. N. Y. Acad. Sci.* 696, 9–19.
- Woolley, C.S., Gould, E., Frankfurt, M., McEwen, B.S., 1990. Naturally occurring fluctuation in dendritic spine density on adult hippocampal pyramidal neurons. *J. Neurosci.* 10, 4035–4039.
- Woolley, C.S., McEwen, B.S., 1992. Estradiol mediates fluctuation in hippocampal synapse density during the estrous cycle in the adult rat. *J. Neurosci.* 12, 2549–2554.
- Woolley, C.S., McEwen, B.S., 1993. Roles of estradiol and progesterone in regulation of hippocampal dendritic spine density during the estrous cycle in the rat. *J. Comp. Neurol.* 336, 293–306.
- Woolley, C.S., McEwen, B.S., 1994. Estradiol regulates hippocampal dendritic spine density via an N-methyl-D-aspartate receptor-dependent mechanism. *J. Neurosci.* 14, 7680–7687.
- Woolley, C.S., Weiland, N.G., McEwen, B.S., Schwartzkroin, P.A., 1997. Estradiol increases the sensitivity of hippocampal CA1 pyramidal cells to NMDA receptor-mediated synaptic input: correlation with dendritic spine density. *J. Neurosci.* 17, 1848–1859.
- Yang, L.C., Zhang, Q.G., Zhou, C.F., Yang, F., Zhang, Y.D., Wang, R.M., Brann, D.W., 2010. Extranuclear estrogen receptors mediate the neuroprotective effects of estrogen in the rat hippocampus. *PLoS One* 5, e9851.

Fig.S1

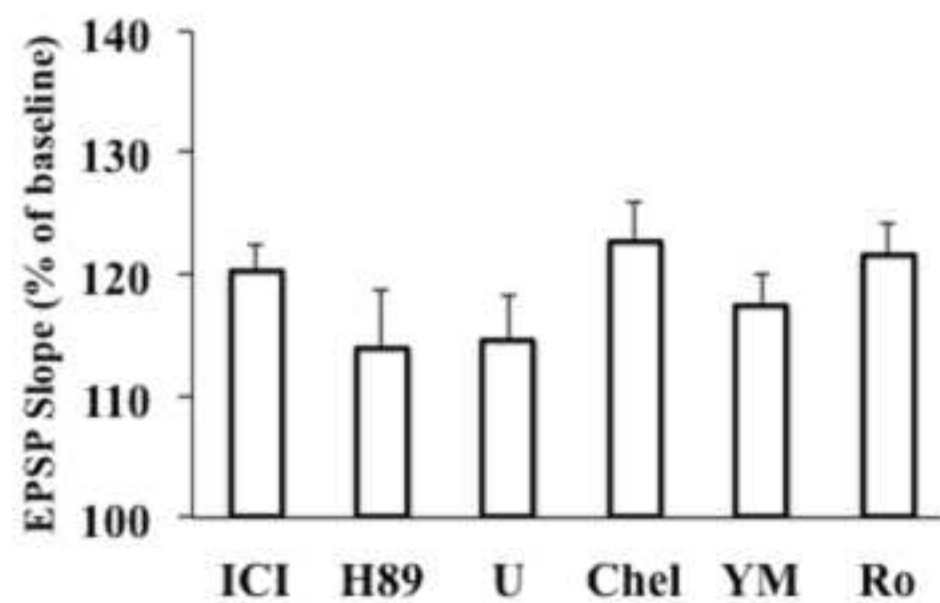


Fig.S2

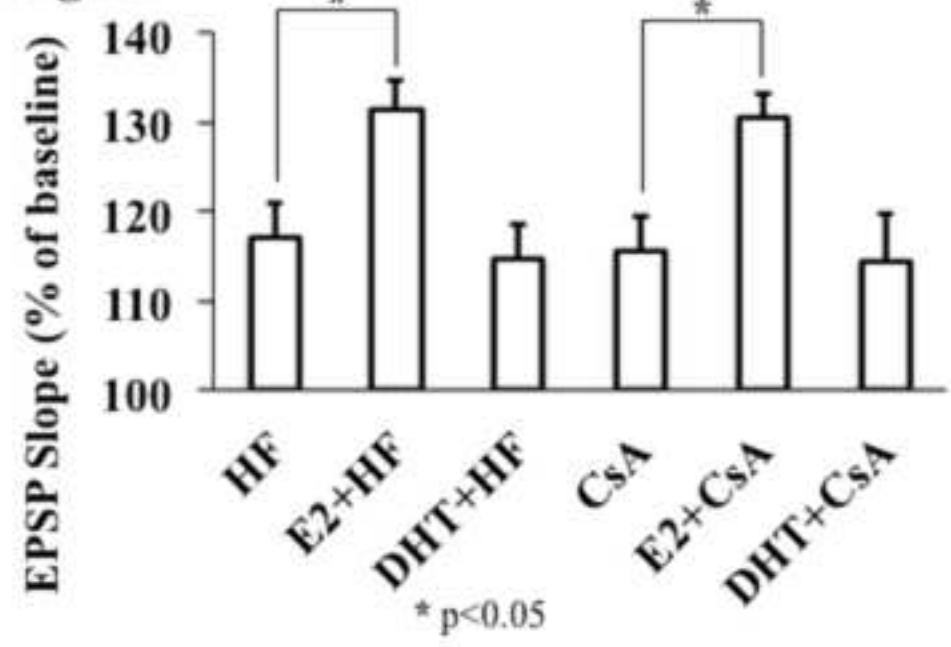


Fig. S3

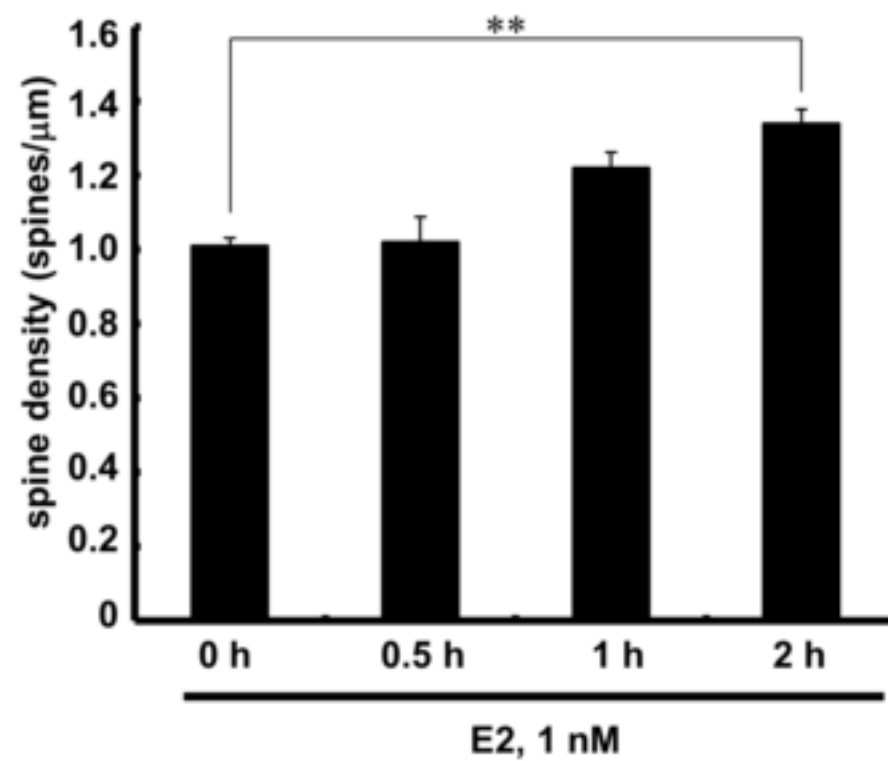
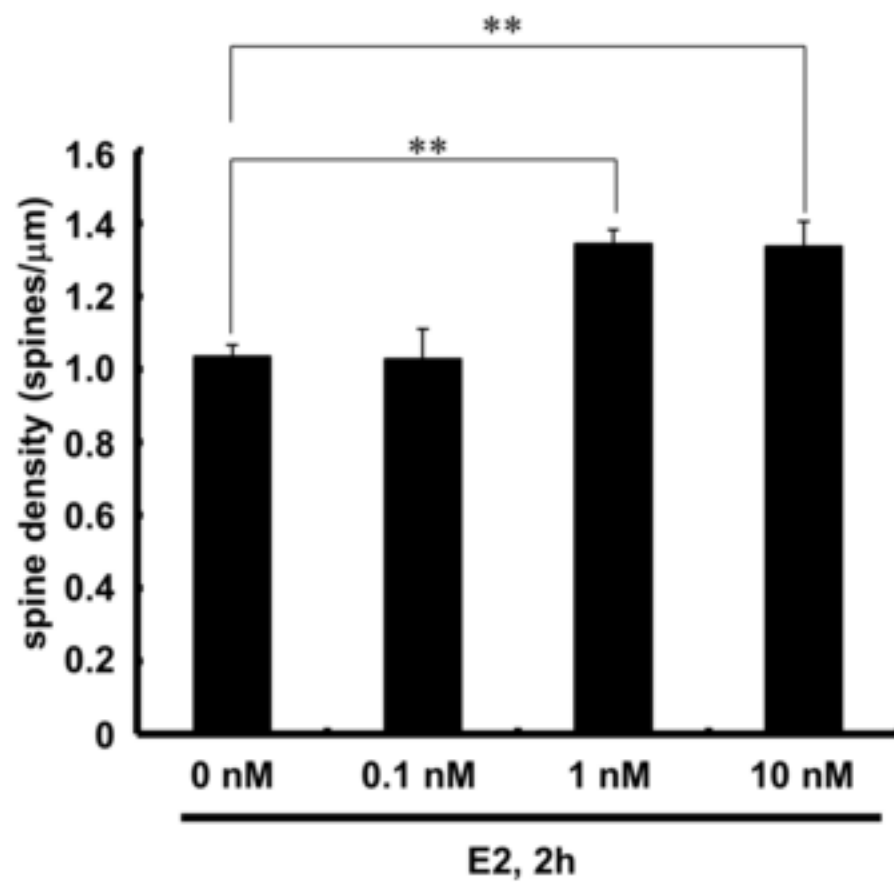


Fig. S4

(A)

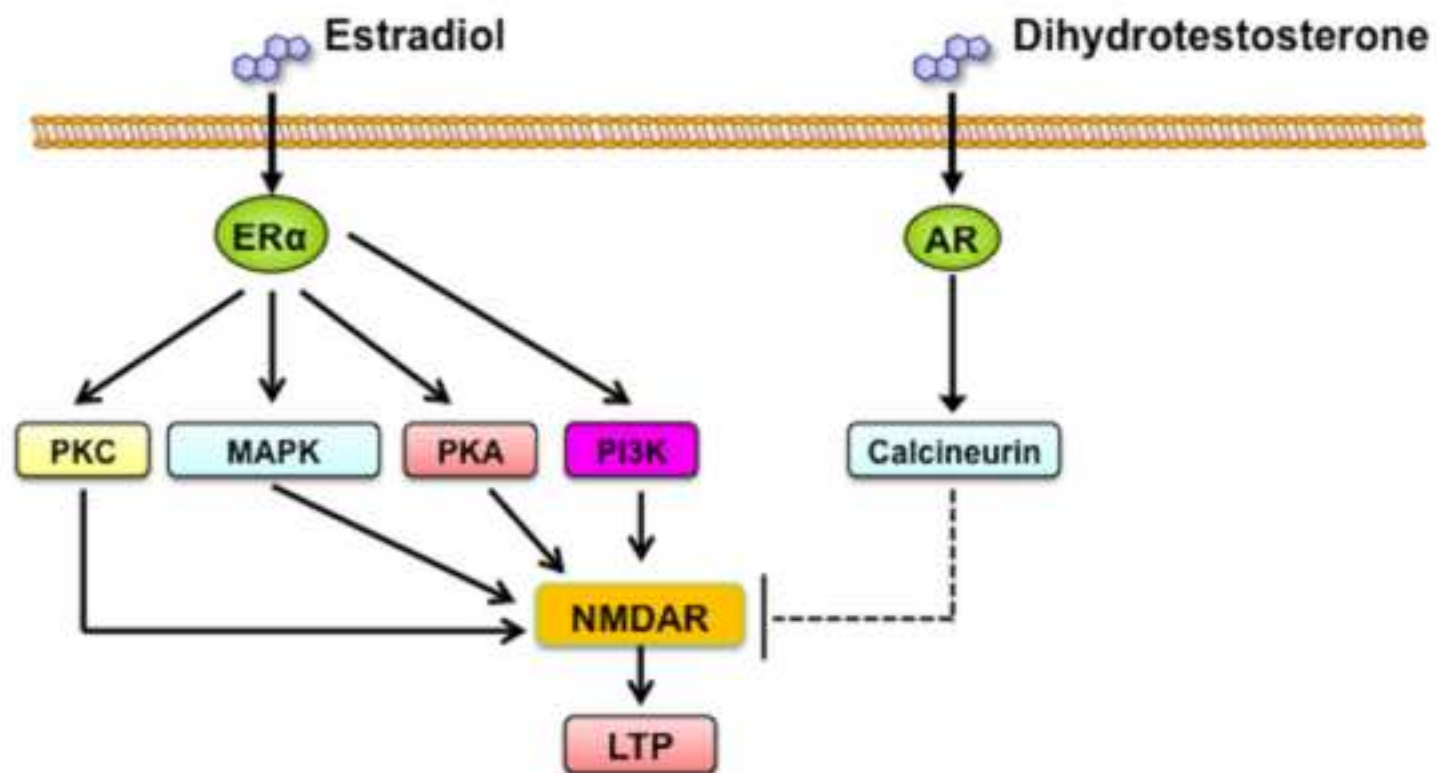
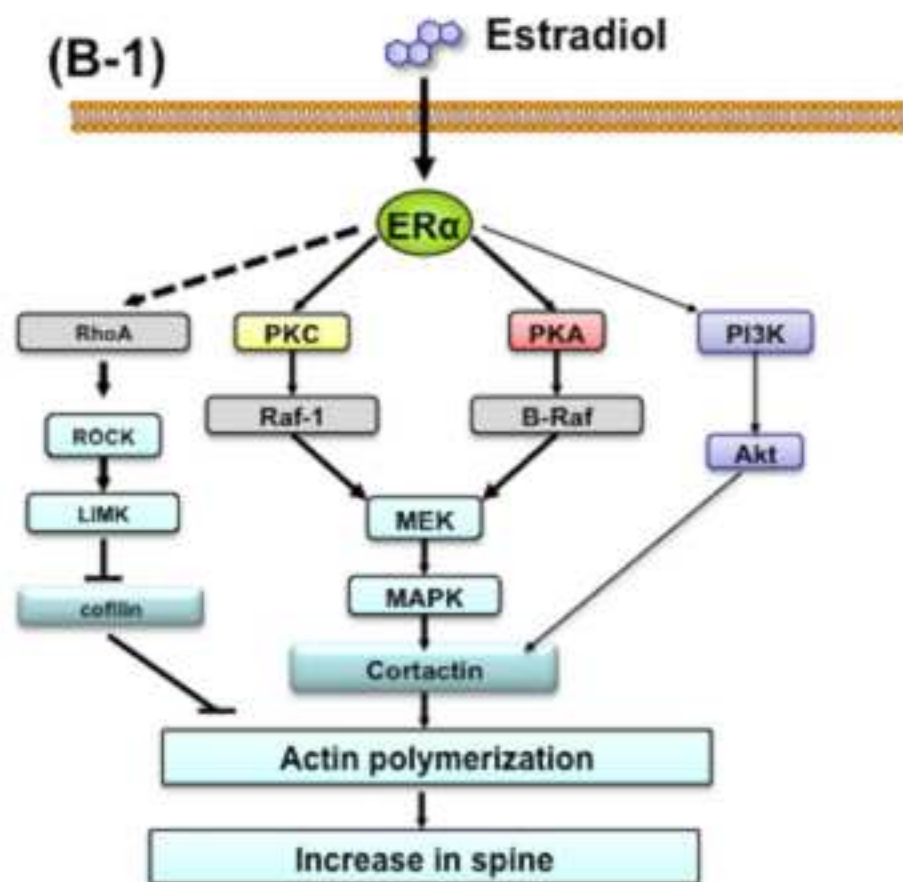


Fig. S4



(B-2) New spine formation (~2 h)

